Nonlinear Dyn (2012) 69:601–614
DOI 10.1007/s11071-011-0290-1

ORIGINAL PAPER

On the effect of nonsmooth Coulomb friction on Hopf bifurcations in a 1-DoF oscillator with self-excitation due to negative damping

Hartmut Hetzler

Received: 5 May 2011 / Accepted: 1 December 2011 / Published online: 7 January 2012
© Springer Science+Business Media B.V. 2012

Abstract This article deals with the question, to what extent damping due to nonsmooth Coulomb friction may affect the stability and bifurcation behavior of vibrational systems with self-excitation due to negative effective damping which—for the smooth case—is related to a Hopf bifurcation of the steady state.

Without damping due to Coulomb friction, the stability of the trivial solution is controlled by the effective viscous damping of the system: as the damping becomes negative, the steady state loses stability at a Hopf point. Adding Coulomb friction changes the trivial solution into a set of equilibria, which—for oscillatory systems—is asymptotically stable for all values of effective viscous damping. The Hopf point vanishes and an unstable limit cycle appears which borders the basin of attraction of the equilibrium set. Moreover, the influence of nonlinear damping terms is discussed.

The effect of Coulomb frictional damping may be seen as adding an imperfection to the classical smooth Hopf scenario: as the imperfection vanishes, the behavior of the smooth problem is recovered.

Keywords Hopf bifurcation · Self-excitation · Non-smooth system · Friction induced vibration · Negative damping · Coulomb damping · Friction damping · Joint damping

H. Hetzler (✉)
Institute of Engineering Mechanics (Institut für Technische Mechanik, ITM), Karlsruhe Institute of Technology (KIT), Kaiserstrasse 10, 76131 Karlsruhe, Germany
e-mail: hartmut.hetzler@kit.edu

1 Introduction

Self-excited vibrations are a common phenomenon in engineering application and cover a huge variety like friction induced vibrations [8, 9, 16, 17, 20] chatter of tool machines ([1, 20, 21] for instance), fluid-structure-interaction problems [3, 11], or oil-whirl of rotors in fluid bearings (e.g., [4, 13, 27, 28]).

In most cases, the self-excited vibrations arise from a steady state, when the corresponding trivial solution loses its stability: thus, the occurrence of these vibrations is related to a Hopf bifurcation. With regard to the engineering problems mentioned before, two main mechanisms leading to instability can be distinguished: negative damping and flutter. In the first case, the basic mechanism is due to a negative effective damping, resulting from forces with a negative gradient with respect to a velocity coordinate (e.g., [11, 18]). For the investigation of the basic character of this mechanism, 1 DoF-systems are sufficient. The second mechanism—usually referred to as flutter, oscillatory instability, modal interaction, or mode coupling—may only appear in systems with at least two degrees-of-freedom. This mechanism is particularly often found in rotating systems [3, 4, 30] or systems involving frictional contacts between deformable bodies [16]. This

latter mechanism will be considered in a separate article.

Apart from self-excitation, another very common phenomenon in engineering applications is nonviscous damping, which often stems from microslip friction or air-pumping in joints and interfaces between members of a system ([2, 26, 29] for instance). As a simple model, Coulomb friction elements may be used to model joint damping (e.g., [12, 29]).

This article investigates the effect of dissipation due to Coulomb friction on steady-state stability and the bifurcation behavior in a one-dimensional system with nonlinear viscous damping and self-excitation due to negative damping. Although such problems can be found in the context of many practical engineering applications, there are only extremely few publications on self excitation in the presence of damping due to Coulomb damping [31, 32].

As a practical example, a model problem with friction excitation is considered; however, the results are not restricted to friction induced vibrations. From an abstract point of view, the frictional-excitation problem under discussion yields a Rayleigh-oscillator with cubic dissipation terms.

2 A 1 DoF model problem: friction induced self-excitation as an engineering example

In the following, the well-known text book example of a mass on a belt (cf. [7, 14] for instance) is chosen to derive a generic equation of motion of a system exhibiting self-excitation due to negative damping. Here, this basic model is extended by additional nonlinear damping terms as well as damping due to Coulomb sliding friction, which may be a simple model to account for joint damping.

The model problem is outlined in Fig. 1: it consists of a simple mass-spring-damper-system, which is pressed onto a conveyor belt; between the mass and the conveyor belt sliding friction is present with a coefficient of sliding friction μ which depends on the relative velocity $v_{\mathrm{rel}} = v_0 - \dot{x}$. The oscillator is subjected to symmetric nonlinear structural damping.

The equations of motion read

$$m\ddot{x} + d_1\dot{x} + d_3\dot{x}^3 + c(x + x_0) + F\mu(v_{\mathrm{rel}}) \in F_R, \quad (1)$$

$$F_R = \begin{cases} -R\,\mathrm{sign}(\dot{x}), & |\dot{x}| > 0 \\ [-R, R], & |\dot{x}| = 0 \end{cases}. \quad (2)$$

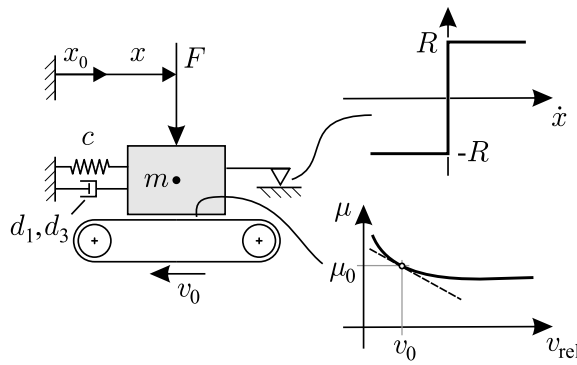

Fig. 1 Model problem: self-excitation due to sliding friction with a coefficient of sliding friction, which depends on the relative velocity

Here, F_R is the convex set valued force of the frictional damping element and system (1) is a differential inclusion of Filippov-type. It is assumed that $\dot{x} < v_0$, so that in the contact between mass and belt stiction will not occur.

Since F_R is upper semicontinuous, convex, closed, and bounded (cf. also Fig. 1) for each initial condition continuous solutions $x(t)$ exist (cf. [6, 10, 24] for instance). Uniqueness of the solution depends on the behavior in the switching plane $\dot{x} = 0$ and will be discussed below.

Assuming small vibration amplitudes, the friction characteristic $\mu = \mu(v_{\mathrm{rel}})$ may be expanded into a Taylor series about v_0

$$\begin{aligned} \mu(v_{\mathrm{rel}}) &= \mu(v_0) + \left.\frac{\partial\mu}{\partial v_{\mathrm{rel}}}\right|_{v_0} \left(\frac{\partial v_{\mathrm{rel}}}{\partial\dot{x}}\right)\dot{x} \cdots \\ &\quad + \frac{1}{2}\left.\frac{\partial^2\mu}{\partial v_{\mathrm{rel}}^2}\right|_{v_0} \left(\frac{\partial v_{\mathrm{rel}}}{\partial\dot{x}}\right)^2 \cdot x^2 + \cdots \\ &= \mu_0 + \mu_1\dot{x} + \frac{1}{2}\mu_2\dot{x}^2 \ldots . \end{aligned} \quad (3)$$

Now, the dimensionless variables $q = x/x_0, \tau = \omega_0 t$ are introduced, where x_0 is the static displacement and $\omega = c/m$ is the eigenfrequency of the undamped linear subsystem. After neglecting all terms of higher than third order and subtracting the static problem, the equation of motion in q reads

$$q'' + 2Dq' + D_2q'^2 + D_3q'^3 + q \in f_R, \quad (4)$$

$$f_R = \begin{cases} -r\,\mathrm{sign}(q'), & |q'| > 0, \\ [-r, r], & |q'| = 0, \end{cases} \quad (5)$$

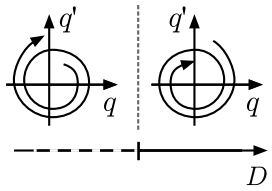

Fig. 2 Stability of the trivial solution for the smooth problem, i.e. for vanishing Coulomb friction ($r = 0$)

where $()'$ denotes differentiation with respect to the dimensionless time τ. The dimensionless damping parameters D, D_1, D_2 and the intensity r of the frictional damping are defined as

$$D = \frac{d_1 + F\mu_1}{2m\omega_0}, \qquad D_2 = \frac{F\mu_2 x_0}{2m}, \tag{6}$$

$$D_3 = \frac{d_3\omega_0 x_0^2 + \frac{1}{6}F\mu_3\omega_0 x_0^2}{m}, \qquad r = \frac{R}{m\omega_0^2}. \tag{7}$$

Within this paper, it is assumed that $|D| \leq 1$, and hence the corresponding linear system is oscillatory.

Introducing the state space vector $\mathbf{z} = (q, v)^\top$ system (5) can be recast in state space form yielding the differential inclusion

$$\mathbf{z}' \in \mathbf{f}(\mathbf{z}) = \begin{bmatrix} v \\ -q - 2Dv - D_2v^2 - D_3v^3 - f_R \end{bmatrix}. \tag{8}$$

Further details on this model problem can be found in [7, 14, 22], for instance, recent investigations on the effect of nonlinear friction characteristics $\mu(v_{\mathrm{rel}})$ may be found in [17, 19].

3 Steady state stability of the smooth subsystem

For $r = 0$, Equation (5) becomes a smooth nonlinear problem, which has the steady state $(q, q') = (0, 0)$. Its stability can be readily assessed by linearizing about the steady state and introducing $q = Ce^{\lambda\tau}$. Eventually, this yields the eigenvalues

$$\lambda_{1/2} = -D \pm j. \tag{9}$$

Obviously, the critical point is at $D = 0$, where the steady state $(q, q') = (0, 0)$ turns unstable as D becomes negative. Since at $D = 0$, vibrations arise from the asymptotically stable steady state; this critical point is a Hopf point (cf. Fig. 2).

4 Steady state stability of the non-smooth problem

For $r > 0$, the problem (5) becomes a nonsmooth nonlinear problem. Steady states with $v = q' = 0, q'' = 0$ are now given by the set of equilibria

$$\mathcal{Q}_S = \{(q, v) \,|\, q \in [-r, r], v = 0\} \tag{10}$$

which is convex and is placed on the q-axis of the (q, v)-state plane.

With $\mathbf{f}^+ = \lim_{v\downarrow 0}\mathbf{f}$, $\mathbf{f}^- = \lim_{v\uparrow 0}\mathbf{f}$ and $\mathbf{n} = [0, 1]^\top$, it can be shown that outside the equilibrium set

$$v = 0 \ \wedge \ |q| > r: \quad \left(\mathbf{n}^\top\mathbf{f}^+\right)\left(\mathbf{n}^\top\mathbf{f}^+\right) > 0 \tag{11}$$

holds, while within this set one finds

$$v = 0 \ \wedge \ |q| < r: \quad \left(\mathbf{n}^\top\mathbf{f}^+\right)\left(\mathbf{n}^\top\mathbf{f}^+\right) < 0. \tag{12}$$

From this, it can be inferred that $\mathcal{Q}_S$ is an attractive sliding mode (although the sliding velocity being zero). Outside of $\mathcal{Q}_S$ trajectories cross the hyperplane $v = 0$ in terms of a transversal intersection (cf. Fig. 3).

As mentioned before, existence of continuous solutions follows from the particular type of the nonsmooth friction force f_R. Since it has been found that the sliding mode is attractive, uniqueness of the trajectories in forward time is also assured [10, 24].

4.1 Geometric considerations concerning stability of the equilibrium set

Due to the nonsmoothness of (5) and the set-valuedness of (10), the stability of the steady state solutions can not be assessed via linearization and eigenvalue analysis about a particular point. However, the definition of Lyapunov stability does not imply using eigenvalue analysis—but is based on geometric considerations, which only demand for comparing the behavior of the investigated solution to solutions starting from within an arbitrarily small δ-vicinity. In order to evaluate this definition, the qualitative behavior of solutions in the vicinity of $\mathcal{Q}_S$ is analyzed. To this end, the small strip $|v| < a$ $(a \ll 1)$ in the vicinity of the set $\mathcal{Q}_S$ is investigated. Within this strip, higher order terms in v may be neglected, yielding

$$q'' + 2Dq' + q \approx \begin{cases} -r\,\mathrm{sign}(q'), & |q'| > 0, \\ [-r, r], & |q'| = 0. \end{cases} \tag{13}$$

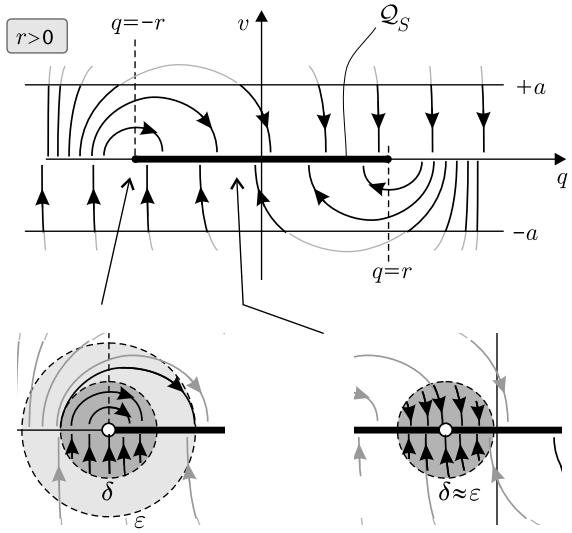

Fig. 3 Qualitative sketch of the phase portrait in the vicinity of the set of steady states $\mathcal{Q}_S$

Using the linear transformations $\tilde{q}^{\pm} = q \pm r$, it is readily found that within the sliding regimes $|v| > 0$ the motion is described by

$$\tilde{q}^{\pm\prime\prime} + 2D\tilde{q}^{\pm\prime} + \tilde{q}^{\pm} \approx 0 \quad \text{for } v \gtrless 0. \tag{14}$$

Hence, within each sliding regime, the solutions to (13) are that of a linear oscillator with linear viscous damping, shifted by r to the left (in upper half-plane) or to the right (in lower half-plane). The corresponding flow is outlined in Fig. 3. Assuming an undercritically damped system (i.e., $|D| < 1$), it is obvious from this sketch that for any point $p \in \mathcal{Q}_S$ a $0 < \delta$-region of admissible initial perturbations can be found in order to keep the perturbations within an ε-region for all times. A similar reasoning for a frictional oscillator without damping can already be found in [15].

In this context, it is remarked that with respect to individual points the set $\mathcal{Q}_S$ is stable but not asymptotically stable. However, if the set $\mathcal{Q}_S$ is seen as a single geometric object, it is asymptotically stable since the solution will end at some point $p \in \mathcal{Q}_S$, and hence the distance to the set $\mathcal{Q}_S$ as a whole converges to zero.

4.2 Analytical stability assessment of the equilibrium set

Beyond this geometric reasoning, LaSalle's invariance principle [14, 23]—which can be extended to non-smooth systems of Filippov-type [25] if they are

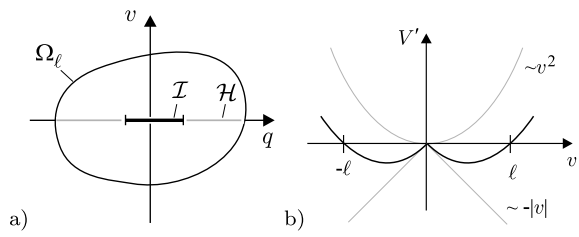

Fig. 4 Asymptotic stability of the equilibrium set: (**a**) Sketch on LaSalle's principle. (**b**) Qualitative outline of V'

unique in forward time—can be applied to prove asymptotic convergence of the set $\mathcal{Q}_S$: Let φ be the flow of a dynamical system and $\varphi(t, \mathbf{z}_0, t_0)$ be a trajectory starting in $\mathbf{z}_0$ at time t_0, being unique in forward time. Suppose $V(\mathbf{z}) \geq 0 \in \mathcal{C}^1$ being a Lyapunov function with $V(\mathbf{0}) = 0$. Assume that

$$\Omega_\ell = \left\{ \mathbf{z} \,|\, V(\mathbf{z}) \leq \ell \wedge V'(\mathbf{z}) \leq 0 \right\} \tag{15}$$

is a compact set where the evolution of $V' = \nabla V^\top \mathbf{f} \leq 0$ under the action of φ is negative or zero and that

$$\mathcal{H} = \left\{ \mathbf{z} \,|\, V'(\mathbf{z}) = 0 \right\} \subset \Omega_\ell \tag{16}$$

is a compact subset where V is stationary ($V' = 0$) and $\mathcal{I} \subset \mathcal{H}$ is the largest positively invariant subset of $\mathcal{H}$, i.e. any solution starting in $\mathcal{I}$ remains in $\mathcal{I}$. Then any trajectory starting in Ω_ℓ (i.e. $\varphi(t, \mathbf{z}_0, t_0)\ \forall \mathbf{z}_0 \in \Omega_\ell$) converges to $\mathcal{I}$ for $t \to \infty$ (cf. Fig. 4a). It may also be concluded that $\mathcal{I}$ must include the datum $\mathbf{x} = \mathbf{0}$.

For the problem under consideration, the invariance principle can be applied since the trajectories are unique in forward time; the hyperplane $v = 0$ corresponds to $\mathcal{H}$ and the subset $\mathcal{Q}_S$ is the largest invariant set within $\mathcal{H}$ (cf. Fig. 4a). From this, it follows that the set $\mathcal{Q}_S$ as a whole is asymptotically stable if one can find an appropriate Lyapunov function V.

Using the total energy $V = \frac{1}{2}q^2 + \frac{1}{2}v^2$ as Lyapunov function, one finds for $v \ll 1$

$$V' = \nabla V^\top \mathbf{f} = [q, v][v, -q - 2Dv - f_R]^\top + h.o.t. \tag{17}$$

$$\approx -2Dv^2 - vf_R = \begin{cases} -2Dv^2 - rv \operatorname{sign} v : |v| > 0 \\ -2Dv^2 + rv[-1, 1] : v = 0 \end{cases} \tag{18}$$

$$= -2Dv^2 - r|v|. \tag{19}$$

The maximum extent of Ω_ℓ defined by (15) is found by demanding $V' \leq 0\ \forall \mathbf{z} \in \Omega_\ell$, yielding

$$v > 0: \qquad V' = v(2Dv + r) \leq 0 \tag{20}$$

$$\rightarrow \quad 0 < v \leq -\frac{r}{2D} = \ell \quad \text{and} \tag{21}$$

$$v < 0: \qquad V' = v(2Dv - r) \leq 0 \tag{22}$$

$$\rightarrow \quad -\ell\frac{r}{2D} < v < 0 \tag{23}$$

as the admissible range of values for v that may be contained by Ω_ℓ. From this, it follows that—for the chosen Lyapunov function—the basin of attraction $\mathcal{A}$ of $\mathcal{Q}_S$ is at least a circle with radius

$$\ell = -\frac{r}{2D} > 0 \tag{24}$$

about the origin (cf. Fig. 4b). Please note that this estimate was found using the linearized equations of motion: Hence, it will only hold if nonlinearities vanish or if they are of negligible magnitude, e.g., for small motions in the immediate vicinity of the equilibrium set. As will be shown later, (24) gives a quite good conservative estimate of the basin of attraction which is induced by the dissipation due to the Coulomb friction. Possible large amplitude limit cycles (e.g., due to other nonlinearities) will be investigated later.

5 Basins of attraction and periodic solutions

As has been indicated by applying Lyapunov's direct method on the linearized problem, the steady state may have a finite basin of attraction for small amplitudes. In the following, it will be investigated if large amplitude basins of attraction exist. Since the problem under consideration is a plane problem, the border of such a basin of attraction must be a periodic solution.

Moreover, for larger amplitudes, the nonlinear viscous damping terms may become relevant and must be taken into account.

5.1 Approximating the attractor of the equilibrium set for the piecewise linear system

In a first step, periodic motions for the piecewise linear system (i.e., $D_2 = 0$, $D_3 = 0$) in the vicinity of the equilibrium set $\mathcal{Q}_S$ are investigated by stitching the piecewise solutions together. This periodic limit cycle will border the basin of attraction of the equilibrium set. The corresponding results hold if nonlinear viscous damping terms are not present or are negligible.

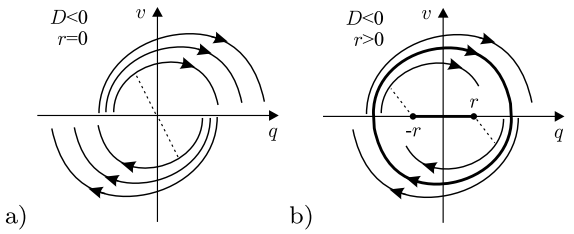

Fig. 5 Qualitative analysis of the dynamics in the phaseplane: (**a**) Smooth system ($r = 0$). (**b**) Nonsmooth system ($r > 0$)

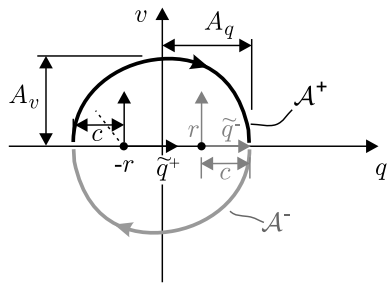

Fig. 6 Construction of a periodic trajectory for the piecewise linear system: $\mathcal{A}^\pm$ are the boundaries of the attractor $\mathcal{A}$ in the upper/lower halfplane

As mentioned before, the phaseportraits in the upper and lower half of the (q, v)-plane correspond to those of the smooth system ($r = 0$), where the upper half is shifted by r to the left and the lower half is shifted by r to the right (cf. Fig. 5b and Fig. 6). For $D < 0$ and $r = 0$, the solutions are spirals of increasing amplitude about the origin—hence, periodic solutions do not exist (cf. Fig. 5a). However, shifting the upper and lower half-planes by $\pm r$ can bring the endpoints of two unstable half-orbits together, which may produce a new periodic solution. Moreover, it is obvious that this periodic solution must have an amplitude that is larger than r since any motion starting within a circle of radius r would be trapped by the attractive set (10) of steady states and, therefore, cannot be periodic.

The basic idea is outlined in Fig. 6: introducing the shift transformation $\tilde{q}^\pm = q \mp r$ (and, therefore, $\tilde{q}^- = \tilde{q}^+ + 2r$) the solutions in the upper and lower halfplane read

$$\tilde{q}^\pm = A^\pm \mathrm{e}^{-D\tau} \cos\omega_d\tau + B^\pm \mathrm{e}^{-D\tau} \sin\omega_d\tau, \tag{25}$$

$$\tilde{v}^{\pm} = \tilde{q}'^{\pm} = -(A^{\pm} D - B^{\pm}\omega_d)\mathrm{e}^{-D\tau}\cos\omega_d\tau \tag{26}$$

$$-(B^{\pm} D + A^{\pm}\omega_d)\mathrm{e}^{-D\tau}\sin\omega_d\tau, \tag{27}$$

where $\omega_d = \sqrt{(1-D^2)}$ is the natural frequency of the damped system and $A^{\pm}$, $B^{\pm}$ are integration constants. The time for one entire cycle would be $T_p = \frac{2\pi}{\omega_d}$. For the problem under consideration, a solution starting within one of the halfplanes immediately at the hyperplane $v = 0$ will reach the hyperplane again after $T = 1/2T_p$.

In order to construct periodic solutions, motions starting at the hyperplane $v = 0$ are considered. Assume a trajectory starting at $\tau = 0$ at $(-c, 0^+)$ with respect to the $(\tilde{q}^+, v)$-system: For these initial conditions, the unknown integration constants for the motion in the positive halfplane read

$$A^+ = -c, \qquad B^+ = -cD/\omega_d. \tag{28}$$

The corresponding constants for the negative plane are easily determined using symmetry. After $\tau = T$, the trajectory reaches the hyperplane again at

$$q^+(T) = c\mathrm{e}^{-D\frac{\pi}{\omega_d}}. \tag{29}$$

Periodic trajectories will be found if $q^+(T) = 2r + c$ holds and from this follows:

$$c = \frac{2r}{\mathrm{e}^{-D\pi/\omega_d} - 1}. \tag{30}$$

With this, the border of the attractor $\mathcal{A}$ is given by the parametric curves

$$\mathcal{A}^{\pm} = \left\{ \left[\begin{array}{l} q_A = r\left(\mp 1 \mp \dfrac{2}{\mathrm{e}^{-D\pi/\omega_d} - 1}\mathrm{e}^{-\frac{D}{\omega_d}\varphi}\cos\varphi \right. \\ \qquad \left. \mp \dfrac{2D}{\omega_d(\mathrm{e}^{-D\pi/\omega_d} - 1)}\mathrm{e}^{-\frac{D}{\omega_d}\varphi}\sin\varphi \right) \\ v_A = \pm\left(r\dfrac{2(D^2+\omega_d^2)}{\omega_d(\mathrm{e}^{-D\pi/\omega_d} - 1)}\mathrm{e}^{-\frac{D}{\omega_d}\varphi}\sin\varphi \right) \end{array} \right], \quad \varphi = 0..\pi \right\} \tag{31}$$

in the (q, v)-system.

The maximum extent of this basin of attraction along q is

$$A_q = r + c = r\left(\frac{\mathrm{e}^{\frac{-D\pi}{\sqrt{1-D^2}}} + 1}{\mathrm{e}^{\frac{-D\pi}{\sqrt{1-D^2}}} - 1}\right) \tag{32}$$

and after some calculus the corresponding maximum extent along v is found as

$$A_v = r\frac{2\mathrm{e}^{-D\pi}}{\sqrt{1-D^2}(\mathrm{e}^{-\frac{D\pi}{\sqrt{1-D^2}}} - 1)} \times \mathrm{e}^{-\frac{D}{\sqrt{1-D^2}}\arctan\frac{\sqrt{1-D^2}}{D}} \times \sin\left(\sqrt{1-D^2} + \arctan\frac{\sqrt{1-D^2}}{D}\right). \tag{33}$$

5.2 First-order approximations for the equilibrium attractor and for periodic motions of large amplitude

For higher amplitudes, the nonlinearities can no longer be neglected: Since exact analytical solutions to the nonlinear problem are not known, approximations for periodic motions must be found.

As mentioned before, the nonsmooth problem (5) is of Filippov-type and due to the particular form of the discontinuous force (convex, upper-semicontinuous) and the fact that the discontinuity produces an attractive sliding mode, existence, and uniqueness of continuous solutions is assured [24]. In general, a continuous periodic solution can be approximated by a Fourier-series. Therefore, assuming solutions which are at least near-periodic, one may try the solution approaches

$$q = A_0 + \sum_{k=1}^{N} A_k\cos(k\eta\tau + \varphi_k), \tag{34}$$

$$v = q' = \sum_{k=1}^{N} -A_k k\eta\sin(k\eta\tau + \varphi_k). \tag{35}$$

This solution approach can be interpreted as a transformation to the new variables (A_k, ψ_k), where $\psi_k = k\eta\tau + \varphi_k$ is the kth phase. These new variable may evolve on a slow time scale.

Differentiation yields

$$q'' = \sum_{k=1}^{N} -A_k k\eta\big(k\eta + \varphi_k'\big)\sin(k\eta\tau + \varphi_k) - A_k' k\eta \sin(k\eta\tau + \varphi_k). \tag{36}$$

In order to obtain compact solutions and motivated by the behavior of the small amplitude solutions (cf. Fig. 7) which tends toward a mostly harmonic limit cycle a first-order series will be used ($N = 1$). Moreover, since (5) is an autonomous system, the choice of the time datum is arbitrary, and hence the phase difference φ_1 can be eliminated. Eventually, this yields the solution approach

$$q = A_0 + A\cos\eta\tau, \qquad q' = -A\eta\sin\eta\tau, \tag{37}$$

$$q'' = -A'\eta\sin\eta\tau - A\eta^2\cos\eta\tau \tag{38}$$

which is the classical Van-der-Pol-transformation.

Inserting (38) into (5), weighting by 1, $\sin\eta\tau$ and $\cos\eta\tau$ and integrating over one cycle yields a system of algebraic equations for the unknowns A_0, A, and η. In doing so, it has been used that the trajectories cross the hyperplane $v = 0$ in terms of a transversal intersection. At these crossings, the friction force for $v = 0$ is finite, nonimpulsive and the time on the hyperplane is a single instant, and hence the corresponding singleton integrals vanish. Eventually, the equations yield

$$\eta = 1, \tag{39}$$

$$A_0 = -\frac{D_2}{2}A^2, \tag{40}$$

$$A' = -\frac{4r}{\pi} - 2DA - \frac{3}{4}D_3A^3. \tag{41}$$

6 Results

In the following, the steady state stability as well as the bifurcation behavior of (5) will be discussed. Since for the smooth problem the steady state stability is controlled by the linear viscous damping, the parameter D will be chosen as bifurcation parameter. Among the remaining parameters r, D_2, D_3, the parameter r will play a prominent role since it controls the transition between the smooth and the nonsmooth problem.

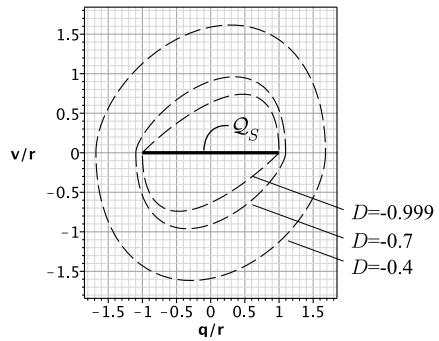

Fig. 7 Basin of attraction for $r > 0$: $D = -0.4$, $D = -0.7$, $D = -0.999$

6.1 Stability of steady states, equilibria sets, and local basins of attraction

For $r = 0$, Equation (5) becomes a smooth problem, which has the steady state point $q_S = (0, 0)$. As the effective viscous damping D changes its sign at $D = 0$, a Hopf Bifurcation occurs: for $D > 0$ the steady state is asymptotically stable, while for $D < 0$ it is unstable.

As has been shown, adding Coulomb friction of intensity r to the problem (5) will turn the single steady state point into the set $\mathcal{Q}_S$ of equilibrium solutions. For $r \downarrow 0$, the problem (5) converges toward the associated smooth problem, and consequently the set $\mathcal{Q}_S$ degenerates to the single steady state point $q_S = (0, 0)^\top$ (see Fig. 15).

For the piecewise linear description—which is valid if the nonlinear damping terms either vanish or are of minor importance due to small amplitudes—the attractor is described by the curve (31), which can be compactly characterized by the maxima (32), (33). Due to the (piecewise) linearity and the periodicity condition, the amplitudes are proportional to the intensity r of the Coulomb friction. Figure 7 shows basins of attraction for three different values of $D < 0$. Figure 8 outlines the maximal displacement A_q and velocity A_v of the basin of attraction as function of D and displays the corresponding projection of the equilibrium set $\mathcal{Q}_S$.

If the nonlinear damping terms may not be neglected (e.g., for larger amplitudes), (39)–(41) can be used as first-order approximants A to describe the amplitudes. Since these approximations have been found via a Galerkin-like procedure—i.e., minimization of the weighted residual, using a first order harmonic approach for the solution—they represent some kind of

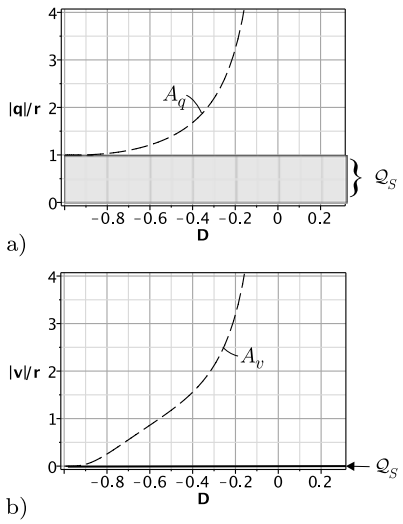

Fig. 8 Maximal extents of the attractor of the equilibrium set $\mathcal{Q}_S$, normalized with the friction intensity r: (**a**) Maximal extent along the displacement axis. (**b**) Maximal extent along the velocity axis

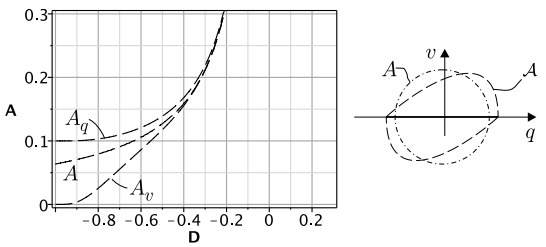

Fig. 9 Basin of attraction $\mathcal{A}$—characterized by A_q and A_v—in comparison to the amplitude A of the first-order harmonic approximation (for example, $r = 0.1$)

average solution. In particular, it is found that A is in between A_q and A_v as the basin of attraction shrinks for $D \downarrow -1$. On the other hand, as the basin of attraction grows for $D \uparrow 0$ A, the amplitudes A_q and A_v of displacement and velocity tend toward the same value. Hence, the approximation A given by (39)–(41) may be used for large amplitudes as well as—in an average sense—for small amplitudes to characterize the size of the basin of attraction: Fig. 9 gives a comparison.

6.2 Limit cycles and basin of attraction

Equations (39)–(41) allow to calculate the mean value A_0 as well as the amplitude A of a harmonic approximation of possible periodic motions. Seeking for stationary amplitudes $A' = 0$, Equation (41) becomes a cubic algebraic equation for A:

$$0 = \frac{4r}{\pi} + 2DA + \frac{3}{4} D_3 A^3. \tag{42}$$

Although this equation could still be solved analytically for A (e.g., using Cardano's method [5]), the results are rather cumbersome and do not allow for an obvious physical interpretation of the parameters.

For this reason, in the following mainly numerical results will be presented. However, some particular points and asymptotes are given in analytical form in order to characterize the solution curves and provide more physical insight.

6.2.1 *Characteristic points & asymptotes*

The theory of cubic equations can be exploited to find characteristic points of the amplitude curve: using the determinant

$$\Delta = -4a^3 - 27b^2 \tag{43}$$

where $a = \frac{8}{3}\frac{D}{D_3}$ and $b = \frac{16}{3\pi}\frac{r}{D_3}$, the following cases can be distinguished:

$$\Delta > 0 \rightarrow 3 \text{ real roots} \tag{44}$$

$$\Delta = 0 \rightarrow 3 \text{ real roots (two belong to a double root)} \tag{45}$$

$$\Delta < 0 \rightarrow 1 \text{ real root, 2 complex roots.} \tag{46}$$

From these roots, only real-valued nonnegative ones are reasonable stationary amplitudes of periodic motions. Further analysis yields

$$\Delta = \frac{1}{3}\left(\frac{16}{3D_3}\right)^2 \left[-8D^2\left(\frac{D}{D_3}\right) - \left(\frac{9}{\pi}\right)^2 r^2\right]. \tag{47}$$

Thus, since $D_3^2 > 0$, $D^2 > 0$, the sign of Δ—and, therefore, the number of solutions—is determined by the sign of bracketed term.

Three different scenarios of physical meaningful amplitudes $A > 0$ can be distinguished (cf. Fig. 10):

- $D_3 > 0$: two amplitudes $A > 0$ for $D < D_F$, no stationary amplitude for $D > D_F$
- $D_3 = 0$: one amplitude for $D \leq 0$ (i.e., $D_F = 0$), no amplitude for $D > 0$
- $D_3 < 0$: one amplitude $A > 0$ for all values of D.

For $D_3 > 0$, the real double root appearing for $\Delta = 0$ marks the border between the region of three and the region of one stationary solution. This border is found at

$$D_F = -\frac{1}{2}\sqrt[3]{\left(\frac{9}{\pi}\right)^2 r^2 D_3}, \tag{48}$$

where the index F indicates that this point belongs to a fold bifurcation of the amplitude. Moreover, determining $D = D(A)$ from (42) and solving $\frac{\mathrm{d}D}{\mathrm{d}A} = 0$ for A yields the corresponding amplitude

$$A_F = \sqrt[3]{\frac{8}{3\pi}\frac{r}{D_3}}. \tag{49}$$

If two solution branches exist, they meet at the fold point $F = (D_F, A_F)$; its position D_F, and hence the number of possible amplitude branches is outlined in Fig. 11.

For the case $D_3 < 0$, the fold point F does not exist: for these cases, the point $Z = (0, A_Z)$ where the solution branches crosses the ordinate can be used to characterize the solution curves. Here, A_Z is given by

$$A_Z = \sqrt[3]{-\frac{16}{3\pi}\frac{r}{D_3}}. \tag{50}$$

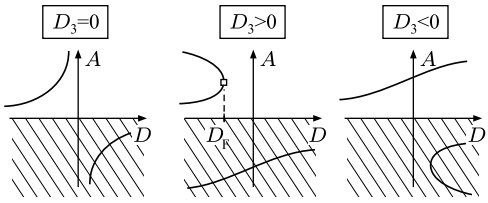

Fig. 10 Possible stationary amplitudes A depending on D and D_3: only positive solutions $A \geq 0$ are physically meaningful (*non-hatched area*)

Assuming small amplitudes and Coulomb friction, which is of the same order of magnitude as the linear part, an approximation to (42) can readily be found. For $\mathcal{O}(\frac{2r}{\pi}) = \mathcal{O}(|DA|)$ and $A^2 \ll |\frac{2D}{3D_3}|$, one finds

$$A_1 \approx -\frac{2r}{\pi D} > 0. \tag{51}$$

For $D_3 = 0$, only one solution branch exists and this equation is the exact solution for any value of $A > 0$. For $D_3 \neq 0$, this equation gives an asymptote for solutions with small amplitude $A^2 \ll |\frac{2D}{3D_3}|$.

Equation (51) gives $A_1 \approx -0.6\frac{r}{D}$ while Lyapunov's direct method yielded $\ell = -0.5\frac{r}{D}$: Obviously, the latter is a very good conservative estimate of the basin of attraction.

Assuming the damping due to Coulomb friction to be very small compared to the remaining part of equation (42), viz. $|\frac{2r}{\pi D}| \ll |A + \frac{8D_3}{3D}A^3|$, yields

$$A_2 \approx \sqrt{-\frac{8D}{3D_3}} \tag{52}$$

as an approximation for large amplitudes.

6.2.2 *Stationary amplitudes*

Using the asymptotes A_1, A_2 as well as the characteristic points A and Z derived before, the amplitude curves can conveniently be described.

For vanishing cubic damping ($D_3 = 0$), only one stationary solution exists, which is given exactly by (51). As can easily be verified, $\frac{\mathrm{d}A'}{\mathrm{d}A}|_{A=A_1} > 0$ holds, and hence this amplitude belongs to an unstable limit cycle. This amplitude gives the border of the basin of attraction of the equilibrium set $\mathcal{Q}_S$. Due to the singularity at $D = 0$, infinitely small Coulomb friction

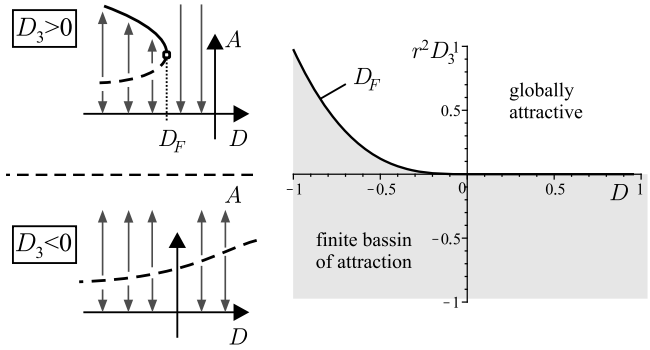

Fig. 11 Extent of the basin of attraction: Equation (48) defines the border between parameter combinations, where the trivial solution is globally attractive, and those where the trivial solution has a finite basin of attraction, bordered by an unstable limit cycle

damping r would be sufficient to stabilize the steady state for small values of $D < 0$.

For progressive cubic damping ($D_3 > 0$), a fold point F appears at (D_F, A_F) (cf. (48) and (49)). For $D < D_F$, two solution branches exists, which asymptotically approach A_1 and A_2 (given by (51), (52)) as D tends toward $D = -1$. From (41), it may easily be concluded that $\frac{\mathrm{d}A'}{\mathrm{d}A}|_{A=A_1} > 0$ and $\frac{\mathrm{d}A'}{\mathrm{d}A}|_{A=A_2} < 0$ and therewith the lower branch A_1 is unstable while the upper one is stable. Obviously, the lower branch borders the basin of attraction of the equilibrium set, while the upper one is a second stationary solution which coexists to the equilibrium set. For $D > D_F$, no periodic motions are found and $\mathcal{Q}_S$ is globally attractive. This scenario is depicted in Fig. 12a.

For $D_3 < 0$, only one stationary amplitude exists: for $D < 0$, the corresponding curve can be approximated by A_1, while for $D > 0$ the asymptote A_2 provides a good approximation; the crossing of the ordinate is given by $Z = (0, A_Z)$. It can easily be verified that these stationary amplitudes belong to unstable limit cycles: thus, they are bordering the basin of attraction of the equilibrium set. This case is outlined in Fig. 12b.

6.3 Mean value shift and asymmetry

Once the amplitude A of the first-order approximation has been determined, the shift of the corresponding mean value can be calculated using (40). Since $A_0 \sim A^2$, it will play no role for small amplitudes $A \ll 1$ but may show some effect for larger amplitudes (cf. Fig. 13).

In the following, asymptotic approximations are given: Equation (51) can be used as an approximation for the lower branch of amplitudes: inserting into (40)

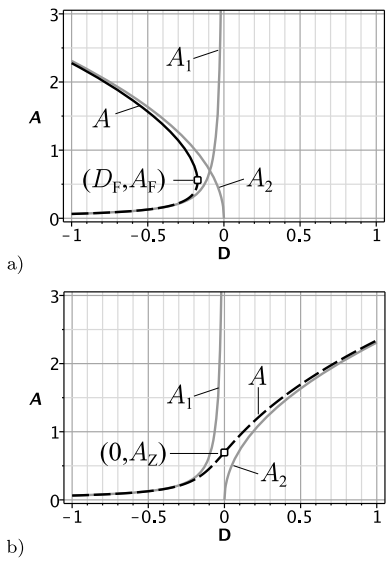

Fig. 12 Schematic amplitude curves including characteristic points and asymptotes: (**a**) $D_3 > 0$: supercritical solution curves A, including the asymptotes A_1,A_2, and the fold-point (D_F, A_F). (**b**) $D_3 < 0$: subcritical solution curve A, including the asymptotes A_1,A_2 and the zero crossing $(0, A_Z)$

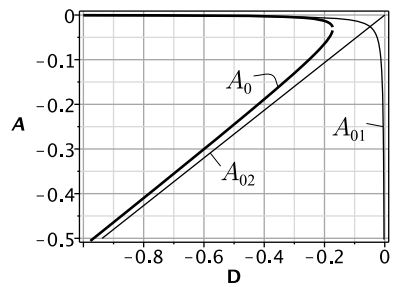

Fig. 14 Shift of mean value A_0 and corresponding asymptotic approximations A_{01}, A_{02}. Numerical example for $D_2 = 0.2$, $D_3 = 0.5$

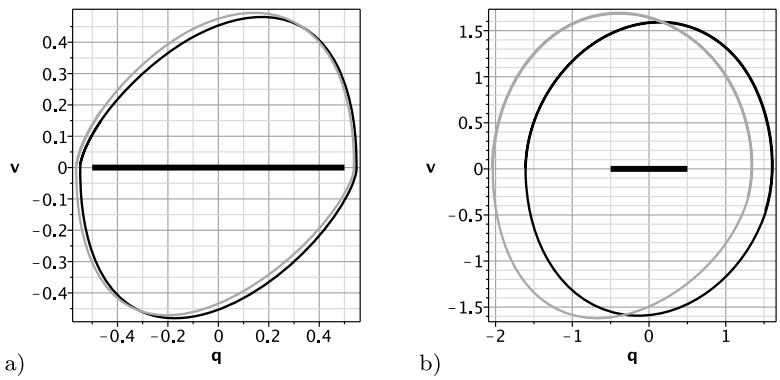

Fig. 13 Effect of asymmetric damping D_2: (**a**) Small amplitudes ($D = -0.7$, $r = 0.5$, $D_3 = 0$). (**b**) Larger amplitudes ($D = -0.2$, $r = 0.5$, $D_3 = 0$)

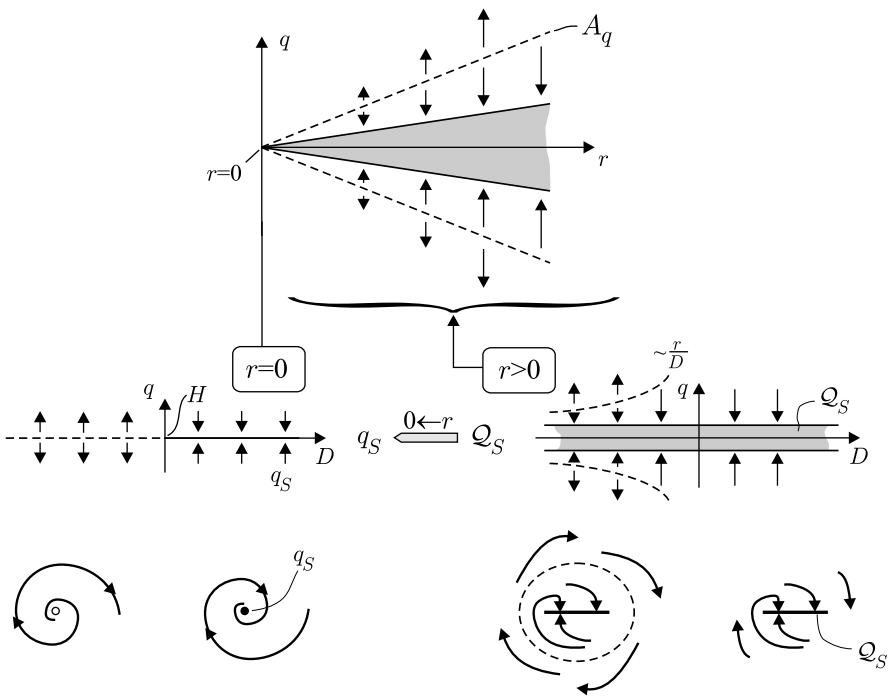

Fig. 15 Steady state and basin of attraction: as $r \to 0$ the equilibrium set $\mathcal{Q}_S$ degenerates to the single point q_S. Simultaneously, the basin of attraction (- -) shrinks to zero size. Note that the basin of attraction in the *right subpanel* holds only for small amplitudes or vanishing nonlinear dissipation

yields

$$A_{01} \approx \frac{2r^2}{\pi} D_2 \frac{1}{D} \tag{53}$$

as an approximation for the mean value shift of the solution branch A_1. For the special case $D_3 = 0$, this is the only solution and holds exactly.

The upper solution branch (existing for $D_3 \neq 0$) may be approximated by (52) and the corresponding approximation of the mean value shift reads

$$A_{02} \approx \frac{4D_2}{3D_3} D. \tag{54}$$

To give an impression, numerical solutions for the first-order approximation shift A_0 as well as the corresponding asymptotes A_{01}, A_{02} are displayed in Fig. 14 for the example $D_2 = 0.2$ and $D_3 = 0.5$.

6.4 Bifurcation behavior

In the following, above results will be summarized with respect to the bifurcation behavior. Motivated by the corresponding smooth system, the effective viscous damping D is chosen as bifurcation parameter. The bifurcation will be investigated by looking at stationary amplitudes and their stability; the shift of the mean value will not be considered since it produces merely a distortion of the phase portrait without changing the general topology (cf. Fig. 13).

For the smooth system ($r = 0$), the steady state is a single point q_S of the phaseplane, which changes its stability as the effective viscous damping changes its sign: at $D = 0$ a pair of conjugate complex eigenvalues crosses the imaginary axis and a Hopf bifurcation takes place.

In the presence of nonlinear dissipative terms, stationary amplitudes may exist: for $D_3 > 0$ the bifurcation at $D = 0$ is a supercritical Hopf bifurcation, and for $D_3 < 0$ the bifurcation at $D = 0$ is a subcritical Hopf bifurcation. For the marginal $D_3 = 0$, no stationary amplitudes apart from the steady state exist. This is a classical Hopf bifurcation for smooth systems and is outlined in the left subpanels of Figs. 15, 16, as well as the upper panel of Fig. 17.

Adding Coulombian frictional damping ($r > 0$) leads to a degeneration of the bifurcation: The stationary point q_S becomes a set $\mathcal{Q}_S$ of stationary points, whose width is proportional to r. In particular, this set is attractive for all values of D. Depending on D and D_3, the basin of attraction is either infinite or finite: This implies that stability assessments may not

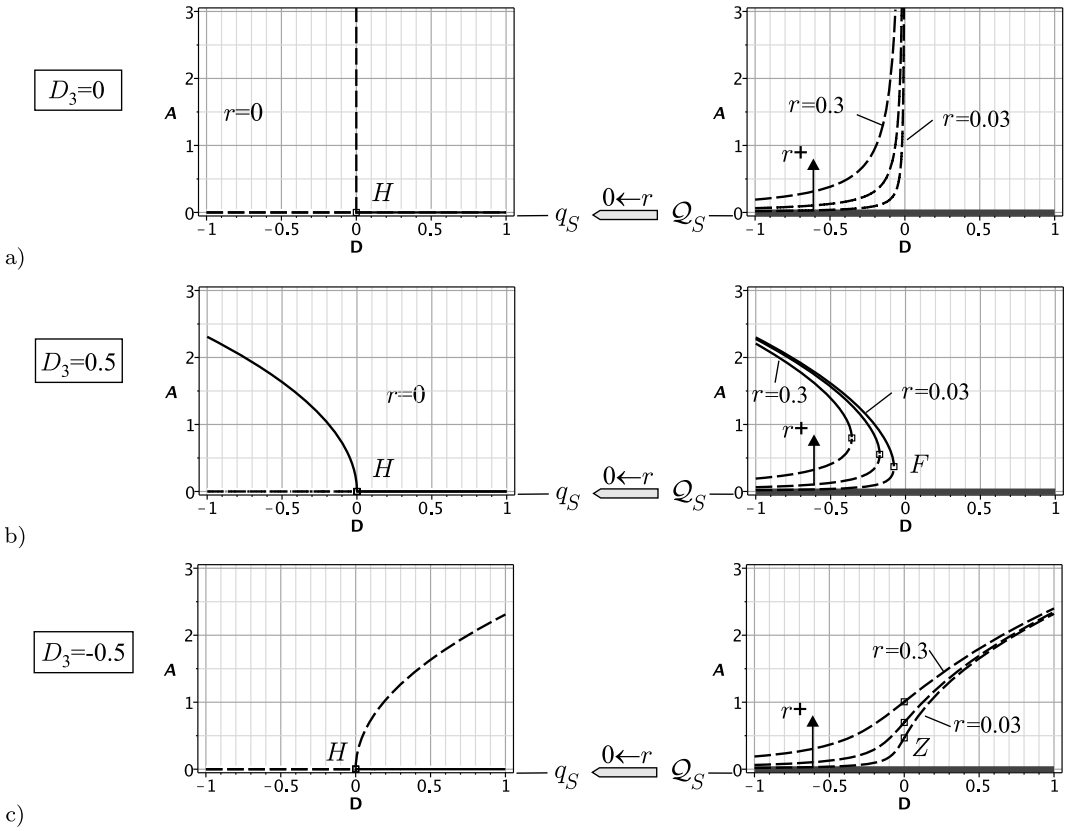

Fig. 16 Bifurcation scenarios for different values of r and D_3: (**a**) Marginal case $D_3 = 0$. (**b**) Supercritical bifurcation. (**c**) Subcritical bifurcation

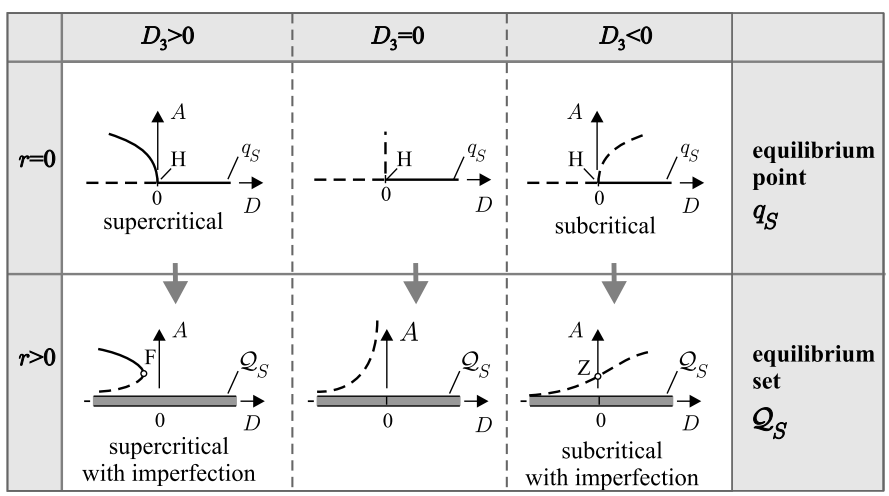

Fig. 17 Overview on the bifurcation behavior

tell whether the steady state is stable or unstable (as is the usual approach for the corresponding smooth system), but will rather make sense in the context of investigating whether particular levels of perturbation are admissible.

Moreover, the Hopf point vanishes and a new unstable limit cycle appears instead, which borders the basin of attraction of the set $\mathcal{Q}_S$. This new limit cycle can be found for $D < 0$ and is induced by the dissipation due to the Coulomb friction.

In the limit $r \to 0$, the set $\mathcal{Q}_S$ degenerates again to the single steady state point q_S and the unstable solution branch (viz. the margin of the basin of attraction) shrinks to size zero: eventually it merges with q_S in the negative half-axis of D and produces the instability of q_S beyond the Hopf point. Simultaneously, the fold point F (for $D_3 > 0$) or the zero crossing Z (for $D_3 < 0$) coalesce with $(0, 0)$ in the bifurcation diagram depicted in Fig. 17, giving birth to the Hopf point H. In this context, the Hopf-point of the smooth problem can be interpreted as a degenerated fold point or zero-crossing point of the nonsmooth problem. The corresponding unfolding is controlled by the parameter r.

Obviously, the strong impact of frictional damping of Coulomb type on small amplitudes is related to the scaling behavior of the corresponding dissipation. While the dissipation of viscous damping terms scales quadratically with amplitude, that of Coulomb friction scales linearly: For this reason, the impact of the latter terms on limit cycles of small amplitude will be much stronger than that of the viscous damping terms. This fact is also reflected by the evolution V' of the Lyapunov function, for which the total mechanical energy had been chosen (cf. Fig. 4 and (19)).

7 Conclusion and outlook

Within this contribution, the impact of damping due to Coulomb friction on a simple oscillator exhibiting self-excitation due to negative damping has been investigated.

The results could be summarized by the following conception: Adding frictional damping of Coulomb type can be seen as adding an imperfection to the classical Hopf bifurcation scenario, which affects mainly the small amplitude behavior in the supercritical parameter range. The large amplitude behavior is mostly preserved.

Moreover, the steady state point changes into a set of equilibria. While the steady state point loses its stability at the critical value of the bifurcation parameter, the equilibrium set is asymptotically stable for all values of the bifurcation parameter—but may have a finite basin of attraction. In the supercritical parameter range, this basin of attraction is induced by the dissipation of Coulomb friction terms while—corresponding to the classical Hopf scenario—in the subcritical parameter range the basin of attraction can either be finite (due to nonlinear viscous dissipation terms) or infinite.

The classical Hopf scenario is recovered as $r \to 0$ and can be seen as a special, degenerated case of the scenario presented here. In the sense of this limit, the Hopf point of the smooth problem can be interpreted as limit of the fold point or a zero-crossing point of the non-smooth problem for $r \to 0$.

From a practical point of view, it is found that the qualitative question of stability is replaced by the need to quantify the size of the basin of attraction and decide whether particular perturbations are tolerable or not.

Further extensions of this work will account for more detailed and realistic models of joint damping. In a next step, the influence of dissipation due to Coulomb friction on flutter-type instabilities in mechanical systems will be investigated.

References

1. Altintas, Y., Budak, E.: Analytical prediction of stability lobes in milling. CIRP Ann. **44**(1), 357–362 (1995)
2. Beards, C.: Damping in structural joints. Shock Vib. Dig. **11**, 35–41 (1979)
3. Bolotin, V., Herrmann, G.: Nonconservative Problems of the Theory of Elastic Stability, vol. 1991. Pergamon Press, Elmsford (1963)
4. Boyaci, A., Hetzler, H., Seemann, W., Proppe, C., Wauer, J.: Analytical bifurcation analysis of a rotor supported by floating ring bearings. Nonlinear Dyn. **57**(4), 497–507 (2009)
5. Bronstein, I., Semendjajew, K., Musiol, G., Mühlig, H.: Taschenbuch der Mathematik. Harri Deutsch Verlag (2008)
6. Deimling, K.: Multivalued Differential Equations. de Gruyter, Berlin (1992)
7. Den Hartog, J.: Mechanical Vibrations. Dover, New York (1985). (Originally published: McGraw-Hill 1956)
8. D'Souza, A., Dweib, A.: Self-excited vibrations induced by dry friction, part 2: Stability and limit-cycle analysis. J. Sound Vib. **137**(2), 177–190 (1990)
9. Dweib, A., D'Souza, A.: Self-excited vibrations induced by dry friction, Part 1: Experimental study. J. Sound Vib. **137**(2), 163–175 (1990)
10. Filippov, A.: Differential Equations with Discontinuous Righthand Sides. Springer, Berlin (1988)
11. Fulcher, L., Scherer, R., Melnykov, A., Gateva, V., Limes, M.: Negative Coulomb damping, limit cycles, and self-oscillation of the vocal folds. Am. J. Phys. **74**, 386 (2006)
12. Gaul, L., Lenz, J.: Nonlinear dynamics of structures assembled by bolted joints. Acta Mech. **125**(1), 169–181 (1997)
13. Genta, G.: Dynamics of Rotating Systems. Springer, Berlin (2005)

14. Hagedorn, P.: Non-linear Oscillations. Clarendon, Oxford (1988)
15. Hahn, W.: Stability of Motion. Springer, Berlin (1967)
16. Hetzler, H.: On moving continua with contacts and sliding friction: Modeling, general properties and examples. Int. J. Solids Struct. **46**(13), 2556–2570 (2009)
17. Hetzler, H., Schwarzer, D., Seemann, W.: Analytical investigation of steady-state stability and Hopf-bifurcations occurring in sliding friction oscillators with application to low-frequency disc brake noise. Commun. Nonlinear Sci. Numer. Simul. **12**(1), 83–99 (2007)
18. Hetzler, H., Schwarzer, D., Seemann, W.: Steady-state stability and bifurcations of friction oscillators due to velocity-dependent friction characteristics. Proc. Inst. Mech. Eng., Proc., Part K, J. Multi-Body Dyn. **221**(3), 401–412 (2007)
19. Hetzler, H., Seemann, W.: Friction induced flutter instability—on modeling and simulation of brake-squeal. Proc. Appl. Math. Mech. **8**(1) (2008)
20. Ibrahim, R.: Friction-induced vibration, chatter, squeal and, chaos; Part I: Mechanics of contact and friction. Appl. Mech. Rev. **47**(7), 209–226 (1994)
21. Insperger, T., Gradišek, J., Kalveram, M., Stépán, G., Winert, K., Govekar, E.: Machine tool chatter and surface location error in milling processes. J. Manuf. Sci. Eng. **128**, 913 (2006)
22. Kauderer, H.: Nichtlineare Mechanik. Springer, Berlin (1958)
23. LaSalle, J., Lefschetz, S.: Stability by Lyapunov's Direct Method (with Applications). Academic Press, New York (1961)
24. Leine, R., Nijmeijer, H.: Dynamics and Bifurcations of Non-smooth Mechanical Systems, vol. 18. Springer, Berlin (2004)
25. Leine, R., van de Wouw, N.: Stability and Convergence of Mechanical Systems with Unilateral Constraints. Springer, Berlin (2008)
26. Maidanik, G.: Energy dissipation associated with gas-pumping in structural joints. J. Acoust. Soc. Am. **40**, 1064 (1966)
27. Muszynska, A.: Whirl and whip–rotor/bearing stability problems. J. Sound Vib. **110**(3), 443–462 (1986)
28. Myers, C.: Bifurcation theory applied to oil whirl in plain cylindrical journal bearings. J. Appl. Mech. **51**, 244 (1984)
29. Popp, K.: Nichtlineare Schwingungen mechanischer Strukturen mit Füge-oder Kontaktstellen. Z. Angew. Math. Mech. **74**(3), 147–165 (1994)
30. Tondl, A.: Some Problems of Rotor Dynamics. Publishing House of the Czechoslovak Academy of Sciences (1965)
31. Tondl, A.: Quenching of self-excited vibrations: effect of dry friction. J. Sound Vib. **45**(2), 285–294 (1976)
32. Yabuno, H., Kunitho, Y., Kashimura, T.: Analysis of the van der Pol system with Coulomb friction using the method of multiple scales. J. Vib. Acoust. **130**, 041008 (2008)